In-silico insights to identify the bioactive compounds of edible mushrooms as potential MMP9 inhibitor for Hepatitis-B

Mishra Divya[1], Chaturvedi Aparna[1], Rashmi Mayank[1] and Singh M.P.[1,2]*
1. Centre of Bioinformatics, Institute of Interdisciplinary Studies (IIDS), University of Allahabad, Prayagraj-211002, INDIA
2. Centre of Biotechnology, Institute of Interdisciplinary Studies (IIDS), University of Allahabad, Prayagraj-211002, INDIA
*mpsingh.16@gmail.com

Abstract
This study aimed to explore effective anti-hepatitis drugs formed from edible mushroom compounds. It is reported that MMP-9 overexpression influences the shielding signaling pathways. The over-expression of MMP9 is due to the hepatitis b virus invasion in peripheral blood vessels, so the disruption of MMP-9 - IFNAR1 interaction is identified as a promising method to expand an anti-hepatitis drug. Mushrooms are attributed as a rich source of phytochemical compounds. The therapeutic efficacy of mushrooms is not well reported against hepatitis-b. We have taken 29 compounds from mushrooms handpicked through literature mining to check the most promising inhibitor against MMP9. We have also calculated the ADME/T property that revealed all 29 compounds with essential pharmacokinetic properties under the acceptable range.

The docking was performed through Glide XP and validated through QPLD XP (Schrodinger, LLC, NY, USA). Based on docking scores and poses, Gerronemin and Hispidin were selected as the most potent inhibitors of MMP9. But based on the docking poses and simulation trajectory analysis, Hispidin showed better stability than Gerronemin. Our results suggest that its efficacy and inhibitory property may cure chronic-Hepatitis B.

Keywords: Matrix metalloproteinase9 (MMP9), Hepatitis-B, Edible Mushrooms.

Introduction

Chronic hepatitis-B also known as liver cancer is mainly caused due to hepatitis viral infection but their mechanism is unknown. According to Chen et al[5], MMP9 (matrix metalloproteinase) regulates the HBV and VSV via inhibiting the activity of IFN and revealing the unique mechanism through which hepatitis virus inhibits the host defensive machinery to establish replication via MMP9 activation. They demonstrated that the hepatitis virus initially induces the host machinery immune response, but the activation is further repressed via MMP9[19]. Thus, the mechanism suggests that MMP9 plays a significant role in the inhibiting interferon signalling pathways in response to hepatitis virus infection.

Also, the MMP9 role has been observed in hepatocellular carcinoma (HCC) invasion, metastasis and hence it is involved in the NF-κB signalling pathway involving protein-protein interactions (PPIs)[13].

On the one hand through the lysosome pathway the MMP9 promotes IFNAR1 destruction whereas phosphorylation and p38 functioning are not mandatory for MMP9 mediated destruction of IFNAR1 response for HBV stimulation. On the other hand, MMP9 aided IFNAR1 destruction in an ERK and TYK2 independent manner. MMP9 belongs to the matrix metalloproteinases (MMPs) family secreted by neutrophils, macrophages and capillary endothelial cells and endopeptidases are responsible for both physiological and pathophysiological tissue remodelling[27]. Currently, 22 members of this family have been described in humans. MMP9 the 92-kDa type IV collagenase or gelatinase-B plays a significant role in the degradation of extracellular matrix (ECM) in a large spectrum that involves tissue remodeling process[16].

The structural analysis of MMP9 reveals that it consists of the catalytic domain, linker domain, NH_2 terminal pro-domain and COOH terminal hemopexin-like domain[20]. The catalytic domain of MMP-9 contains two zinc ions, five calcium ions and three repeats homologous to the type II module of fibronectin. One of the two zinc ions of the catalytic domain is essential for its proteolytic activity and hence ECM degradation. Therefore, it has been focused upon exclusively in the work. Only the catalytic domain has been discussed here, unlike other disciplines that may have a role in the active site of MMP9.

In this study, we have focused on investigating the therapeutic effects of edible mushroom high and low molecular weight compounds using various computational approaches including molecular docking, ADME/T analysis, QM-polarized ligand docking and molecular dynamic simulation. The first screening was performed for low and high molecular weight compounds present in mushrooms as a potent MMP9 inhibitor[6,17,21]. In the course of inhibition of MMP9, several medicinal mushroom extracts were reported as an excellent natural source[22].

Some of the examples of LMW edible mushroom compounds are hydroquinone, (E)-2-(4-hydroxy-3-methyl-2-butenyl)-hydroquinone and polyporenic acid C isolated from *Piptoporus betullinus* (commonly known as birch polypore)[1,15]. Hispidin belonging to the catechol-family

isolated from *Phellinus linteus* shows anti-viral immunomodulating properties[13]. Several triterpenes from *Ganoderma lucidium* such as ganoderic acid are active as antiviral agents against human immunodeficiency virus type 1[7].

Also, gerronemin isolated from the extracts of *Gerronema sp*. and gliotoxin isolated from *Gliocladium fibriatum* to name a few are examples of HMW compounds. Likewise, polyporenic acid C and lanostane compounds were also extracted from another mushroom i.e. Daedalea dickinsii both reported compounds found as a natural inhibitor source against MMP9[4]. We have taken 29 compounds which were handpicked through literature mining and compounds were available in PubChem database[10,11,13,23]. Secondly, docking was performed for top-ranked compounds with MMP9[12,24]. At the last, molecular dynamics simulation was used to check the stability and comparison of a complex of selected compounds with MMP9 protein[2].

Material and Methods

Selection of compounds and ADME/T property prediction: In this work, we have taken 29 compounds of edible Mushrooms. The ADME/T properties were calculated by QikProp which predicts the required principle and physiochemical descriptors of selected compounds[25]. The program was processed in normal mode predicted principle descriptors and physiochemical properties for all known and searched compounds with detailed analysis of the log*P* (octanol/water), QP% (human oral absorption). It also evaluates the acceptability of the entire known and searched compounds based on Lipinski's rule of 5 which is necessary for rational drug design[23].

Macromolecule preparation: The three-dimensional structure of MMP9 protein of *Homo sapiens* with best resolution at 1.104 Å corresponding to PDB ID:6ESM was downloaded from Protein Data Bank. The protein was further modified for Glide docking calculations and subjected to protein preparation using the Prep wizard program of Schrödinger-Maestro (Schrodinger, LLC, New York, NY, USA). Likewise, four steps used in this process that is all hydrogens were removed, assigned bond orders, added all the missing side chains and added required hydrogens for heavy atoms. All the water molecules within 5Å region of protein were retained that might be taking part in active site and the rest were removed.

Progressively weaker restraints were applied for the non-hydrogen atoms. Using OPLS_2005 force field, progressive minimizations were performed until the average root mean square deviation of the non-hydrogen atoms reached 0.3 Å[14]. This refinement procedure was carried out based on the recommendations of Schrodinger LLC (New York, NY, USA).

Compounds preparation for screening: All the twenty-nine HMW and LMW compounds (Table 1) have been reported to be inhibitors against 6ESM derived from edible mushrooms. The structures of compounds downloaded from Pubchem database in SDF file-format were incorporated into Maestro workspace (Schrodinger, LLC, New York, NY, USA). Each structure was assigned an appropriate bond order using the LigPrep package. The ionization states were generated at pH7.0±2.0 using Epik program. Epik can automatically be employed by LigPrep to enumerate tautomers and protonation states in Schrödinger Suite. The inhibitors were optimized by means of the Optimized Potentials for Liquid Simulations (OPLS3e) force field.

Receptor grid generation: Receptor grids were calculated for prepared protein such that various ligand poses bind with the predicted active site during docking. In Glide, grids were generated through the default parameters i.e. van der Waals scaling factor 1.00 and charge cut-off 0.25 subjected to OPLS_2005 force field. A cubic box of specific dimensions around the centroid of the active site residues was generated for the receptor. The dimensions of centroid of active site were -1.781Å, 49.254Å and 21.041Å for x, y and z coordinates respectively as also inspected with the help of PDBeMotif an active site prediction tool availed by EMBL-EBI. The dimensions of box were set to 10 Å × 10 Å × 10 Å for docking experiments.

Extra precision (XP) docking and QM-polarized ligand docking (QPLD): All the HMW and LMW mushroom compounds as well as native ligand (PCID: 133084111) were subjected to Glide XP docking. Initially, an extra precision (XP) Glide docking was carried out[33]. On the other hand, for QM/MM calculations, Quantum polarised ligand docking (QPLD) approach uses the QSite program which is coupled with JAGUAR for the QM region[3]. These two approaches were used to get more insights into the interaction of selected compounds and protein active site regarding accuracy. The QM/MM energy is calculated as the Coulomb–van der Waals force of the complex calculated from the electrostatic potential energy of the ligand.

The final energy evaluation is done with the Glide score and a single best pose is generated as output for a particular ligand with the help of the following equation:

$$\text{Gscore} = a * \text{vdW} + b* \text{Coul} + \text{Lipo} + \text{Hbond} + \text{Metal} + \text{BuryP} + \text{RotB} + \text{SiteGScore}$$

where vdW = van der Waal energy, Coul = Coulomb energy, Lipo = Lipophilic contact term, Hbond = Hydrogen-bonding term, Metal = Metal-binding term, BuryP = Penalty for buried polar group, RotB = Penalty for freezing rotatable bonds, SiteGScore = Polar interaction at active site and the coefficients of vdW and Coul are $a = 0.065$ and $b = 0.0130$[33].

The choice of the best-docked structure for each ligand was made using model energy score (emodel) that combines Glide score, the non-bonded interaction energy and the excess internal energy of the generated ligand conformation.

Table 1
List of edible mushroom derived compounds acting as MMP9 inhibitors

S.N.	Organisms Name	PubChem CID	Compound name	SMILES
1	*Tricholoma matsutake*	3973	LY-294002	N1(C=COC=C1) C1=CC(=C2[C@H](O1)/C(=C/1\C=CC=CC1)/CC=C2) O[32]
2	*Phellinus linteus*	54685921	Hispidin	o1c(cc(cc1=O) O)/C=C/c1cc(c(cc1)O)O[32]
3	*Cordyceps melitaris*	6303	Cordycepin	o1c(c(cc1CO) O) n1c2ncnc(c2nc1)N[8]
4	*Ganoderma lucidium*	14109375	Lucidenic acid (A, B, C and N)	O[C@@]12[C@@]34[C@@]56[C@@]14[C@]6(O)C[C@@]14[C@]65/C(=C/5\[C@]73[C@@]38[C@@]7(O5)[C@H]8C=C5[C@]78C3=C2[C@@H]8[C@H]7O5)/[C@]16C/C/4=C\CC(=O)O[16,22]
5	*Hericium erinaceus*	1117189	JNJ0966	s1c(c2nc(sc2) Nc2c(cccc2) OC) c(nc1NC(=O) C) C[30]
6		8051	2-Heptanone	CCCCCC(=O) C[29]
7		14496	Cyclobutanone	C1CC(=O) C1[25]
8		15655	Cyclopropane	C1CC1[25]
9		10341	2(5H)-Furanone	C1C=CC(=O) O1[25]
10		713	Formamide	C(=O) N[25]
11	*Pleurotus ostreatus*	753	Glycerin	C(C(CO)O) O[25]
12		31246	4-Heptanone	CCCC(=O) CCC[25]
13		867	Propanedioic acid	C(C(=O) O) C(=O) O[25]
14		938	Niacin	C1=CC(=CN=C1) C(=O) O[25]
15		79083	1,4-Pentanediol	CC(CCCO)O[25]
16		102848	2-Pyrrolidinone	C1CC(=O) NC1[25]
17		181561	5-Methoxypyrrolidin-2-one	COC1CCC(=O) N1[25]
18		5364452	2-Undecene	CCCCCCCCC=CC[25]
19		53232	Lovastatin	O(c1c2c(c(ccc2cc(c1) C) C)/C=C/c1oc(=O) cc(O)c1) C(=O)/C(=C/C)/C[25]
20	*Lentinus edodes*	159961	Eritadenine	O([C@@]12[C@]34/C/1=C/1\[C@]56c7c3c(C=C(C(=C24)O)C=O) cc(c7C[C@H]5[C@H]16)C)[C@H]1OC=C(C(=C1)O)O[25]
21	*Lentinus sqquarrosulus*	442469	1,2-dihydroxy mintlactone	O1c2c(O)c(ccc2C(=C) C1=O) CO[18]
22	*Piptoporus betulinus*	785	Hydroquinone	Oc1ccc(O)cc1[24]
23	*Calvatia gigantea*	4696	Clavacin	O1[C@@H] (C2=CC(=O) OC2=CC1) O[15]
24	*Lentinus crinitus*	10130519	Panepoxydone	O1C2=C(C=C(C(=O) [C@@H]12)/C(=C/C(=C)C)/O)O
25	*Gliocladium fibriatum*	6223	Gliotoxin	S1SCN(CCO)C2=Nc3c([C@H]4O[C@@]124) cccc3OCO[35]
26	*Ganoderma lucidium*	471002	Ganoderic acid	OC1=C[C@@]23[C@]45[C@]61[C@@]17[C@H]6[C@]7(C6=C7[C@@]89[C@@]%101/C(=C\4/[C@]25C/C/3=C\c1occ(c1)C(=O)O)/O[C@]8%10[C@H]9C=C1[C@]27[C@@H]([C@@H]62)O1)O[35]
27	*Gerronema sp.*	643728	Gerronemin A	Oc1c(cccc1O)/C=C/C=C/C=C/C=C/C=C/C=C/C=C/C=C/c1c(c(ccc1) O) O[7]
28	*Grifola frondosa*	444679	Ergosterol	CC(=C(C)/C=C/[C@H]1C[C@@]23[C@]41C=C/C/1=C/5\CC=C6C=C(O)C=C7[C@]86[C@]65[C@]78/C/6=C\3/[C@@]241)C[35]
29	*Lepiota Americana*	72725	2-Aminophenoxazin-3-one	c12c(n(cn2) C2=CCC(=C2) CO) nc(nc1N=C1CC1) N[35]

QPLD calculation is a time-consuming process, so as a validation approach, the best two docked compounds were selected for QPLD analysis with extra precision (XP) Glide docking[3]. It generates five poses per docked molecule; these were then submitted to QM-ESP charge calculation at the B3LYP/3-21G level within the protein environment defined by the OPLS2005 force field. Finally, the resulting poses were re-docked for another Glide run using the ESP atomic charges and XP scoring modes. QPLD docking gives more accurate treatment of electrostatic interactions which helps to improve the docking accuracy.

Binding free energy calculation: Prime/MM-GBSA was used to predict the binding free energy between the receptor and the set of ligands for the poses obtained from Glide extra precision (XP) docking. Also, the calculation was done for

native ligand re-docked into the active site of MMP9 through Glide XP docking. The binding free energy (ΔG_{bind}) was calculated using the default parameters of prime software, Schrodinger, LLC, New York, NY, USA. The MM-GBSA was used for re-scoring of QPLD analysis to predict the ligand energy, receptor energy and to check any kind of distortions for the poses that were obtained from QPLD analysis considering the electrostatic interaction[22].

MM-GBSA is used to estimate relative binding affinity for selected compounds (reported in kc al/mol). It is a physics based method that computes the force field energies in implicit solvent of the bound and unbound molecules involved in the binding process. Hence, it includes facets such as protein-ligand van der Waals contacts, electrostatic interactions, ligand de-solvation and internal strain energies.

Molecular dynamic simulation: MD simulation has been performed using Desmond program, Maestro, Schrödinger, New York, NY, 2019. On the basis of MM-GBSA score[35] and Lipinski rule[23], the top two docked score compounds were obtained after Glide (XP) docking. It was subjected to solvent-explicit, all-atom molecular dynamics simulations, as a considerable energy difference between both compounds was observed along with difference in their interaction pattern within the active site of MMP9. Nine sodium ions were added as counter ions to neutralize the system; along with it 0.15M NaCl salt concentration was added. A predefined explicit solvent model TIP3P was used and the complex was solvated with 10Å water orthorhombic box.

Prior to the MD simulation, volume minimization was carried out. Further, considering the system as isothermal-isobaric (NPT) ensemble class and keeping the temperature of the system at 300K, pressure is at 1.01325 bar. Each molecular dynamic production run was carried out for 10.0ns while the recording interval was set to 10.0ns for the trajectory and 1.2ns for energy with all other options kept as default.

Results and Discussion

ADME/T property analysis: The drug-like activity of the selected HMW and LMW edible mushroom compounds was categorized using ADME/T properties shown in table 2. Two descriptors have been selected for the ADME/T properties i.e. principle and physiochemical descriptors. The principle descriptors include molecular weight, molecular volume, H-bond donors, H-bond acceptors and their position according to Lipinski's rule of five. The physiochemical descriptors include log P (octanol/water), total solvent accessible surface area and MDCK (Madin-Darby canine kidney) cell permeability.

Lipinski's rule of 5 is the rule of thumb to evaluate drug-likeness; if a chemical compound contains certain pharmacological and biological properties, then properties would make it an active drug[23]. The rule describes molecular properties important for a drug's pharmacokinetics in a living system including ADME/T properties. These compounds were further evaluated for their drug-like behaviour through analysis of pharmacokinetic parameters required for absorption, distribution, metabolism and excretion/toxicity (ADME/T).

The partition coefficient (QPlogPo/w), critical for estimation of absorption within the body as shown in fig. 4(b) ranged between -0.78 and 5.92. QPPMDCK ranges from 1.93 to 254.10. Overall, the percentage of human oral absorption for the compounds ranged from 34.46 to 90.75%. All these pharmacokinetic parameters are within the acceptable range defined for human use, thereby indicating their potential as drug-like molecules.

Glide XP docking and binding analysis: The HMW and LMW compounds were compared on the basis of estimated ΔG as well as docked poses in the MMP9 active site. The residues involved in active site pocket were GLN186, LEU187, LEU188, ALA189, HIS190, GLN227, HIS230, HIS236, LEU243, TYR245, PRO246, MET247, TYR248, ARG249 and THR251. The results corresponding to Glide XP docking for top-ranked ten compounds followed by total binding energy of Prime/MM-GBSA have been shown in table 3. Glide XP docking generated many poses for each compound, therefore, the best Emodel score for the poses was selected for corresponding compounds. Also, the correlation between Emodel score and docking yielded a statistically significant correlation coefficient with R^2 of 0.65 (Fig. 1)[22]. This statistical significance drives the reliability more towards Glide XP docking.

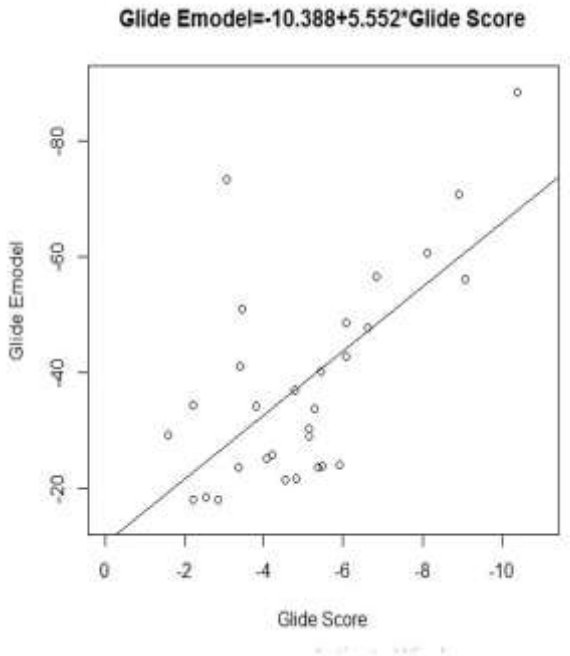

Fig. 1: Correlation between Glide score and Glide Emodel energy.

Table 2
Principal and Physiochemical descriptors listed of Mushroom compounds.

Compound name	Principal Descriptors							Physiochemical descriptors			
	Molecular weight[a]	Molecular volume[b]	vdW[c] PSA	HB[d] donors	HB[e] acceptors	Rotatable bonds[f]	RO5	QPlog Po/w[g]	QP%[h]	SASA[i]	QPP MDCK[j]
LY-294002	412.57	1508.33	83.82	4	3	18	0	5.92	90.75	855.46	98.44
Hispidin	246.22	788.17	105.28	3	4.75	6	0	0.69	64.19	483.44	28.53
Cordycepin	253.17	751.38	155.90	4	8.40	7	0	-0.78	34.46	448.70	1.93
Lucidenic acid (A, B, C and N)	212.21	673.95	74.95	1.5	4.5	1	0	1.14	82.51	416.68	254.10
JNJ0966	307.34	983.56	47.72	0	4.7	1	0	3.41	100	549.85	157.30
2-Heptanone	251.24	760.62	119.78	4	9.1	4	0	-0.99	56.02	452.87	36.41
Cyclobutanone	458.59	1376.91	136.73	2	9.7	5	0	2.77	65.63	700.02	8.16
Cyclopropane	360.44	1101.79	75.69	2	6.75	4	0	3.27	100	641.27	2587.71
2(5H)-Furanone	114.18	566.10	29.10	0	2	4	0	1.54	100	368.90	1665.91
Formamide	70.09	35034	33.19	0	2	0	0	.014	88.10	251.82	1237.49
Glycerin	86.09	374.54	50.20	1	2	1	0	0.58	73.21	264.54	139.50
4-Heptanone	84.07	331.33	42.49	0	3	0	0	-0.55	82.39	234.24	992.21
Propanedioic acid	45.04	230.39	66.08	2	2.5	0	0	-1.58	54.96	185.12	130.61
Niacin	92.09	384.01	67.96	3	5.1	5	0	-1.19	65.51	270.54	159.54
1,4-Pentanediol	114.18	569.38	27.34	0	2	4	0	1.74	100	372.40	2344.53
2-Pyrrolidinone	104.06	368.67	101.12	0	2	2	0	0.37	42.69	262.19	2.99
5-Methoxypyrrolidin-2-one	123.11	447.61	62.54	1	3.5	1	0	0.67	69.03	301.09	72.56
2-Undecene	104.14	481.27	44.48	2	3.4	5	0	-0.02	81.48	323.08	565.82
Lovastatin	99.13	428.83	43.79	1	2.5	0	0	-0.26	76.92	290.72	827.29
Eritadenine	115.13	445.30	53.97	1	4.2	1	0	-0.76	71.84	295.68	694.22
1,2-dihydroxy mintlactone	154.29	791.46	0	0	0	7	0	5.82	100	496.33	5899.29
Hydroquinone	404.54	1298.73	87.24	1	6.7	7	0	4.25	100	671.28	334.38
Clavacin	198.21	660.31	81.38	2	5.45	2	0	0.29	77.56	396.04	253.60
Panepoxydone	110.11	423.94	45.08	2	1.5	2	0	0.79	84.60	289.87	448.04
Gliotoxin	154.12	470.36	73.65	1	5.9	1	0	-0.70	82.50	303.02	72.93
Ganoderic acid	210.22	702.85	82.11	1	6.4	4	0	0.32	79.29	415.91	315.45
Gerronemin A	326.38	883.46	94.48	1	9.4	3	0	-0.80	62.79	495.01	493.15
Ergosterol	516.67	1559.92	157.01	3	11.4	8	0	2.91	49.66	793.41	4.77
2-Aminophenoxazin-3-one	396.65	1406.11	22.49	1	1.7	5	0	7.16	100	736.25	1829.59

[a]Molecular weight of the molecule (accepted range: 130.0–725.0)
[b]Total solvent-accessible volume in cubic angstroms using a probe with a 1.4 A ˚ radius (acceptable range: 500.0–2000.0)
[c]van der Waals surface area of polar nitrogen and oxygen atoms (accepted range: 7–200)
[d]Estimated number of hydrogen bonds that would be donated by the solute to water molecules in an aqueous solution (range: <5)
[e]Estimated number of hydrogen bonds that would be accepted by the solute from water molecules in an aqueous solution (accepted range: <10)
[f]Number of non-trivial (not CX3), non-hindered (not alkene, amide, small ring) rotatable bonds (accepted range: 0.0–15)
[g]Predicted octanol/water partition co-efficient log p (acceptable range: -2.0 to 6.5)
[h]Percentage of human oral absorption (acceptable range:25% is poor and 80% is high)
[i]Total Solvent Accessible Surface Area in using a probe with a 1.4 radius (acceptable range: 300–1000)
[j]Predicted apparent MDCK cell permeability in nm/s

Table 3
GLIDE and Prime/MM-GBSA molecular docking score of mushroom compounds.

Compound name	Glide Score	Glide Emodel	MM-GBSA
Hispidin	-8.929	-70.820	**-74.98**
Gerronemin A	-10.384	-88.453	**-71.66**
Lovastatin	-3.441	-51.048	-66.37
JNJ0966	-3.608	-73.515	-66.05
2-Undecene	-1.569	-29.253	-65.72
Ganoderic acid	-6.621	-47.760	-63.17
Gliotoxin	-3.788	-34.11	-55.84
Lucidenic acid	-6.08	-42.731	-54.38
Panepoxydone	-5.439	-40.081	-51.30
Clavacin	-4.899	-32.206	-49.13

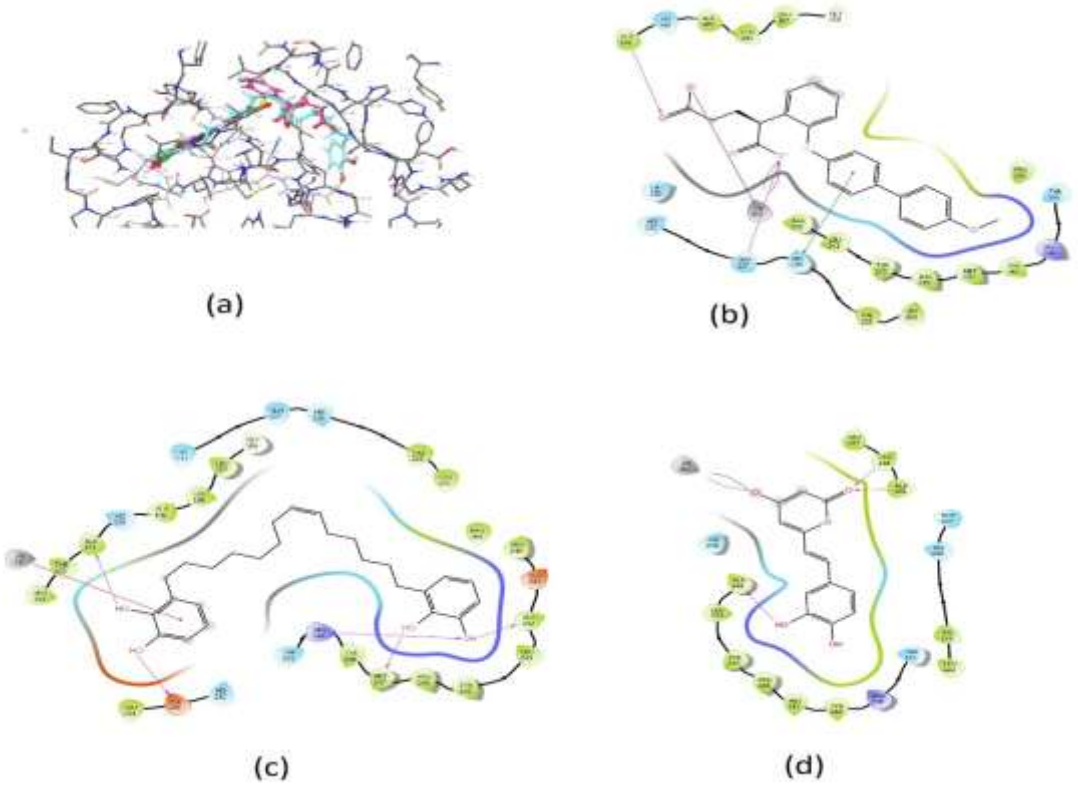

Fig. 2: (a) Native ligand, Gerronemin and Hispidin interation into active site.Two-dimensional interaction diagram of Glide XP docked conformation of the (b) native, (c) Gerronemin and (d) Hispidin into the active site of MMP9. H-bond interactions shown through violet arrow, green line shows π-π interaction, blue-red line for salt-bridge interaction and red line for pi-cation interaction between ligand and active site residues.

On the basis of MM-GBSA score, it can be suggested that the hispidin (PCID: 54685921) was the top-ranked compound amongst all with ΔG value as -74.98 kcal/mol. The MM-GBSA binding energy is calculated using the equation below:

$\Delta G_{binding} = E_{complex} - E_{protein} - E_{ligand}$

where $E_{complex}$ denotes energy of complexed ligand within the active site of mmp9, $E_{protein}$ and E_{ligand} denote individual energies of protein and ligand respectively. The energy in each case includes terms such as protein-ligand van der Waals contacts, electrostatic interactions, ligand desolvation and internal strain (ligand and protein) energies.

Further, the compounds were ranked on the basis of ΔG as obtained from Glide docking score, that considers the binding affinity of the complex only which suggests gerronemin (PCID: 643728) to be the top-ranked compound with value -10.384 kcal/mol. Hence, further the binding pattern of both the compounds into the active site of MMP9 was analysed which has been shown in fig. 2.

As can be observed through fig. 2(a), the amino acid residues involved in native ligand binding are HIS226 making a π-π interaction with the benzene ring of the native ligand whereas GLN227 and ALA191 are involved in hydrogen bond; also metal ion of MMP9 has been observed to be making two salt bridge interactions as well as a metal-coordinate bond with the native ligand. Thus, its high free energy value of -101.54 kcal/mol as obtained through Glide XP re-docking is followed by MM-GBSA calculation.

The three-dimensional interaction of the compounds into the active site of MMP9 shows ZN301 found to be a part of the catalytic domain of the protein to be involved into a pi-cationic interaction with the benzene ring of Gerronemin whereas the hydroxyl groups of phenol group of gerronemin were found to be involved in five hydrogen-bond interaction with amino acid residues ALA191, ASP235, ALA242, MET247 and ARG249 Fig. 2(b). These residues were also observed in the interaction of native ligand with the protein structure into its co-crystallized form as obtained from PDB.

Further, hispidin was observed to be forming a salt-bridge with ZN301 of catalytic domain of MMP9 active-site along with three hydrogen-bond interaction between hydroxyl groups of phenol group of hispidin with amino acid residues LEU188, ALA189 and ALA242. Therefore, we observed that Gerronemin showed better interaction as compared to hispidin Fig. 2(c).

A deep insight into the interaction pattern of the compounds gerronemin and hispidin into the active site of MMP9 revealed much similarity with that of the native-ligand binding pattern in its co-crystallised form (PDB ID: 6ESM). Glide uses Emodel for pose selection which is a more significant weighting of force field components (electrostatic and van der Waals energies) and making it well-suited for comparing conformers. Gerronemin was the best compound on the basis of Emodel energy with value -88.453 and hispidin was the next with value -70.82.

QPLD XP docking and binding analysis: Further, to get more insight into the interaction pattern of these compounds as well as their interaction energies, taking quantum mechanics calculations into consideration as the target protein contained metal atom as necessary for its catalytic activity. QPLD was performed with XP mode of docking results shown through table 4 and interaction in fig. 3.

QPLD results suggested hispidin to have better interaction with MMP-9 active site residues, as it also had least hydrogen-bond energy of -0.14 kcal/mol along with the ligand energy -99.086 kcal/mol that might be responsible for its stability into the active site of the protein. Also, the interaction of gerronemin shows four hydrogen bonds between active site residues and hydroxyl groups as well as a π-π stacking between TYR248 and benzene ring of gerronemin [Fig. 3(a-b)] whereas for hispidin, three hydrogen bonds with active site residues, a salt bridge with ZN301 of catalytic domain of protein and one π-π stacking to benzene ring with HIS226 residue has been observed [Fig. 3(c-d)]. Thus, hispidin is to be involved in better interaction with MMP-9 active site and suggesting for better inhibition as compared to gerronemin or other compounds.

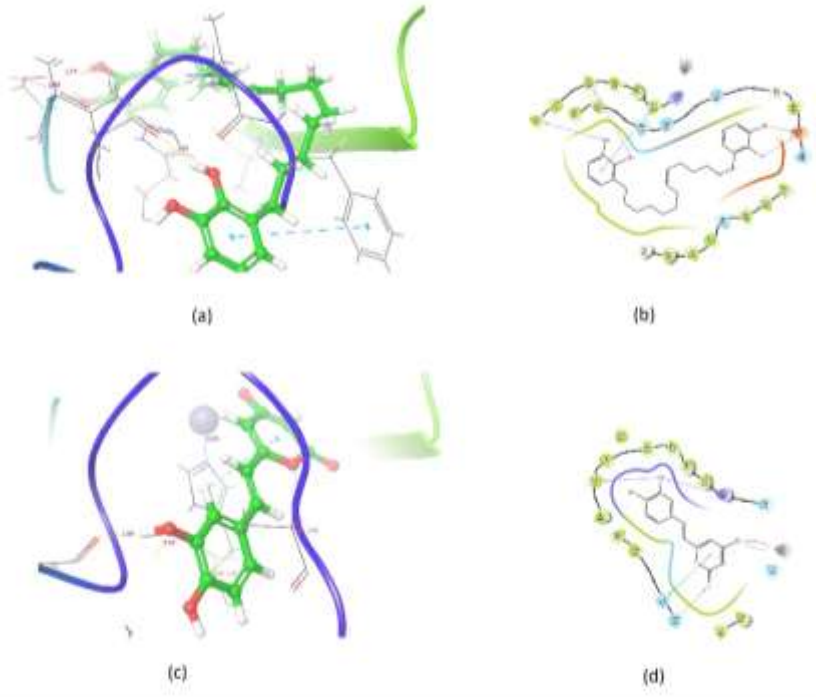

Fig. 3: Three-dimensional interaction diagram of QPLD XP docked conformations of (a) Gerronemin (green, ball-stick representation) and (b) Hispidin (green, ball-stick representation) into the active site of MMP-9 (ribbon representation). H-bond interactions shown through violet and yellow and blue-dotted line shows π-π interaction.

Table 4
QPLD score of top 2 docked compounds obtained through molecular docking using Glide followed by re-scoring of Prime/MM-GBSA. (Add more compound's results).

Compound name	Docking score	Receptor energy	Ligand energy	Prime H-bond
Hispidin	-9.484	-13.044	-99.086	-0.14
Gerronemin A	-5.263	-13.044	-33.593	0.00

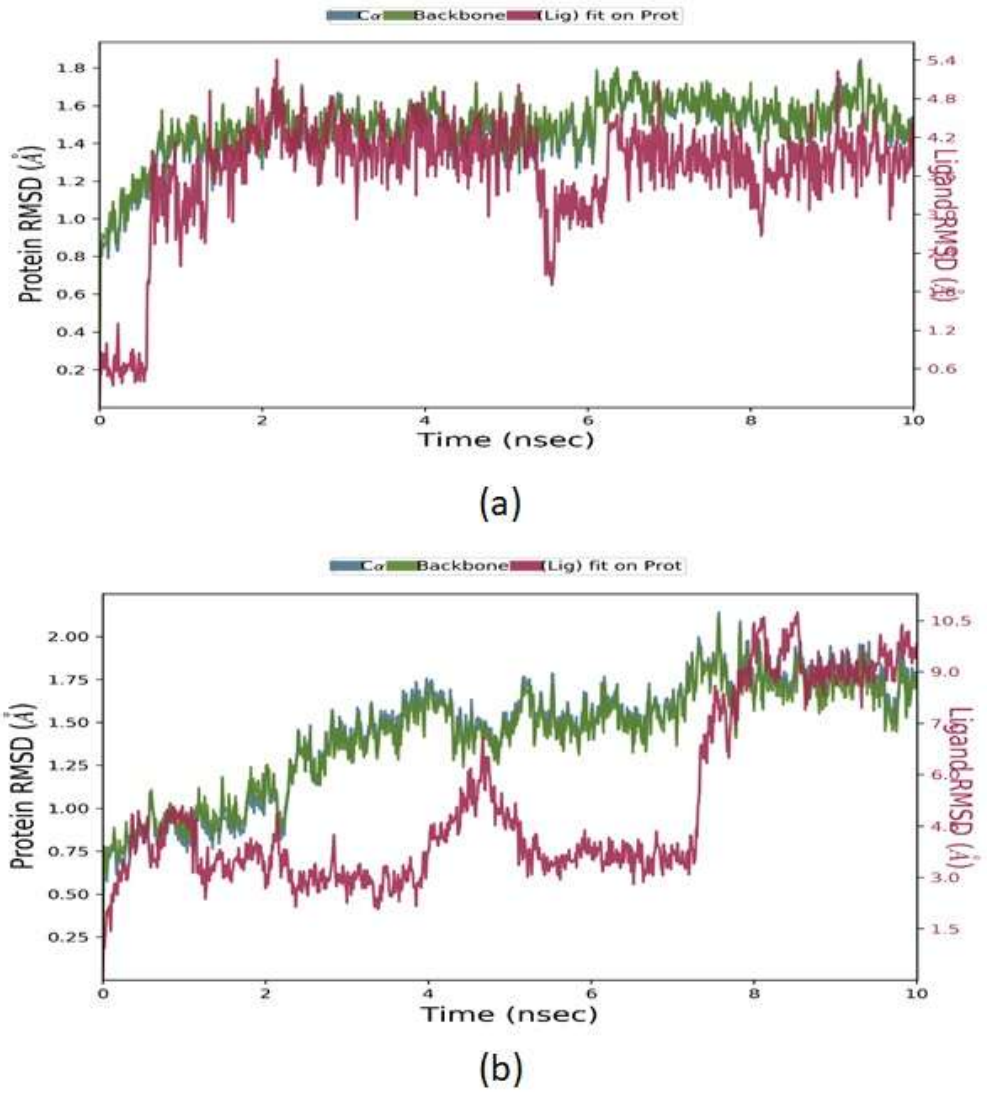

Fig. 4: Protein-ligand RMSF for (a) Gerronemin and (b) Hispidin over 10ns MD simulation.

MD simulation analysis: Molecular dynamics can be used to account for conformational flexibility of protein as well as the ligand molecule and structural stability of the ligand moiety into the active-site of the protein. The complexes of gerronemin and hispidin were analysed with the help of MD simulations for the backbone atoms and the Cα-helix of the protein. The time dependence of the protein-ligand root mean square fluctuation (RMSF) (Å) of the backbone has been shown in fig. 4.

The Root Mean Square Fluctuation (RMSF) is useful for characterizing local changes along the protein chain. The result of MD simulation over the cause of 10ns were not well complying with the backbone RMSF of protein as much fluctuation and hence instability could be observed till 8ns. One of the reasons expected behind this instability of gerronemin into the active-site of MMP9 was due to 18 number of torsions. Further, it was performed for Hispidin-protein conformer and proved to be quite stable for the course of 10ns of MD simulation.

The protein root mean square fluctuation has been shown in fig. 5 along with protein-ligand contacts for both the compounds. It was interesting to see that none of the compounds exceeded beyond 3Å of fluctuation, as can be seen by the peaks in the graph.

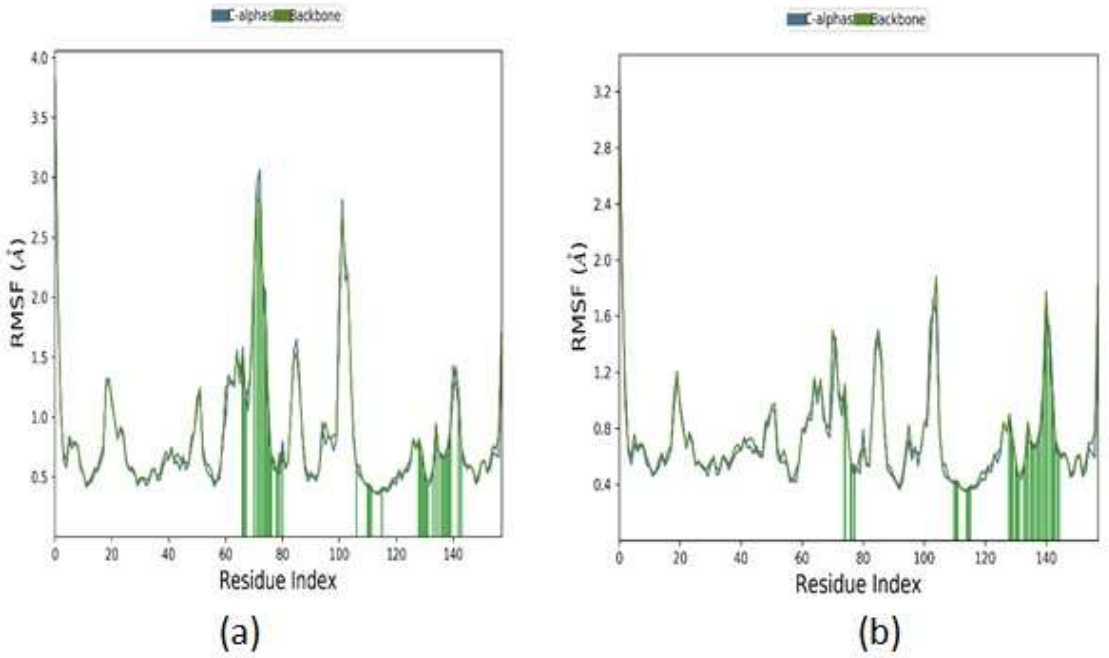

Fig. 5: Protein- RMSF along with ligand contacts (green) for (a) Gerronemin and (b) Hispidin over 10ns MD simulation

It was also observed that the tails (N- and C-terminal) fluctuated more than any other part of the protein. Secondary structure elements like alpha helices and beta strands are usually more rigid than the unstructured part of the protein and thus fluctuated less than the loop regions.

However, the RMSF of protein-ligand as well as MMP9 individually shows instability in case of gerronemin than hispidin. Therefore, hispidin appears as a more stable and intractable to the active site of MMP9. It represents better inhibition towards MMP9, thus acting as a cure for chronic Hepatitis-B.

Conclusion

In conclusion, first through molecular docking and simulation of mushroom compounds were presented as a potential MMP9 inhibitor. In this work, we performed different docking approaches to analyse the interaction of LMW and HMW[32] compounds to MMP9.

Glide XP docking suggested that these mushroom compounds have same binding mode as those of MMP9 active site residues. The results also suggested that the interacting result stabilizes the drug on the active site. Hispidin and gerronemin are the most suitable compounds amongst all. On the other hand, when Glide XP docking results were validated for top four compounds through QPLD XP docking, hispidin was found to be the most suitable bioactive compound followed by gerronemin. It had also shown further good bioactivity when conformational analysis of the compounds was done. Interestingly, on further analysis for getting an insight into the interaction patterns of these compounds along with H-bond, pi-pi stacking as well as pi-cationic interaction with ARG249, a positively charged amino acid residue, were observed.

Moreover, a divalent metal cation Zn^{+2} was further observed which has been reported to play an important role in the stabilization of lead molecules in the active sites of MMP9. The correlation data for Emodel energy and docking score produced considerable statistical significance proving reliability of the results obtained through Glide XP docking. Additionally, ADME properties analysis including physicochemical descriptors and pharmacokinetic parameters are within the acceptable range defining for human use thereby indicating their potential as a drug like molecules.

Hence, on comparing the two bioactive compounds i.e. hispidin and gerronemin, which one will be a better bioactive compound on the active site of MMP9 inhibiting its activity? The trajectory analysis and the flexibility of proteins showed gerronemin to be comprised of 18 Torsions which define too much flexibility on the active sites of MMP9. In contrast hispidin with only five torsions proved to be a relative stable compound, thus proving its efficacy as a bioactive compound and thereby inhibiting the activity of MMP9, hence a potential lead molecule for curing Hepatitis-B.

Acknowledgement

DM gratefully acknowledges fellowship from the University Grants Commission, India.

References

1. Alves M.J., Froufe H.J.C., Costa A.F.T., Santos A.F., Oliveira L.G., Osório S.R.M. and Ferreira I.C.F.R., Docking studies in target proteins involved in antibacterial action mechanisms:

Extending the knowledge on standard antibiotics to antimicrobial mushroom compounds, *Molecules,* https://doi.org/10.3390/molecules19021672, **19**, 1672–1684 **(2014)**

2. Alonso H., Bliznyuk A.A. and Gready J.E., Combining docking and molecular dynamic simulations in drug design, *Medicinal Research Reviews*, https://doi.org/10.1002/med.20067, **26**, 531–568 **(2006)**

3. Bochevarov A.D., Harder E., Hughes T.F., Greenwood J.R., Braden D.A., Philipp D.M. and Friesner R.A., Jaguar: A high-performance quantum chemistry software program with strengths in life and materials sciences, *International Journal of Quantum Chemistry*, https://doi.org/10.1002/qua.24481, **113**, 2110–2142 **(2013)**

4. Borah D., Gogoi D. and Yadav R.N.S., Computer Aided Screening, Docking and ADME Study of Mushroom Derived Compounds as Mdm2 Inhibitor, a Novel Approach, *National Academy Science Letters*, https://doi.org/10.1007/s40009-015-0366-4, **38**, 469–473 **(2015)**

5. Chen J., Xu W., Chen Y., Xie X., Zhang Y., Ma C., Yang Q., Han Y., Zhu C., Xiong Y., Wu K., Liu F., Liu Y. and Wu J., MMP-9 facilitates hepatitis B virus replication through binding with IFNAR1 to repress IFN/JAK/STAT signalling, *Journal of Virology,* DOI: 10.1128/JVI.01824-16, **91 (2017)**

6. Cui M., Mihaly M., Hong-Xing Z. and Meng X.Y., Molecular Docking: A powerful approach for structure-based drug discovery, *Current Computer-Aided Drug Design,* https://doi.org/10.2174/157340911795677602, **7**, 146–157 **(2011)**

7. Chen N.H., Liu J.W. and Zhong J.J., Ganoderic acid T inhibits tumor invasion *in vitro* and *invivo* through inhibition of MMPxpression, *Pharmacological Reports*, **62**, 150-16 **(2010)**

8. Chakrabarti S., Zee J.M. and Patel K.D., Regulation of matrix metalloproteinase-9 (MMP-9) in TNF-stimulated neutrophils : novel pathways for tertiary granule release is rapidly released following stimulation, *J Leukoc Biol.*, https://doi.org/10.1189/jlb.0605353, **9 (2005)**

9. Dash R., Hosen S.M.Z., Karim M.R., Kabir M.S.H., Hossain M.M., Junaid M., Islam A., Paul A. and Khan M.A., In silico analysis of indole3-carbinol and its metabolite DIM as EGFR tyrosine kinase inhibitors in platinum resistant ovarian cancer vis a vis ADME/T property analysis, *J App Pharm Sci*., **5(11),** 073-078 **(2015)**

10. Friedman M., Chemistry, Nutrition and Health-Promoting Properties of Hericium erinaceus (Lion's Mane) Mushroom Fruiting Bodies and Mycelia and Their Bioactive Compounds, *J. Agric. Food Chem.*, **63**, 7108−7123 **(2015)**

11. Ferreira I.C.F.R., Vaz J.A., Vasconcelos M.H. and Martins A., Compounds from Wild Mushrooms with Antitumor Potential, *Anticancer Agents in Medicinal Chemistry*, 10, 424–436 **(2010)**

12. Grinter S.Z. and Zou X., Challenges, Applications and Recent Advances of Protein-Ligand Docking in Structure-Based Drug Design, *Molecules*, **19**, 10150–10176 **(2014)**

13. Huang G.J., Huang S.S. and Deng J.S., Anti-Inflammatory Activities of Inotilone from *Phellinus linteus* through the Inhibition of MMP-9, NF-κB and MAPK Activation *In Vitro* and *In Vivo*, *PLoS One,* **7**, e35922 **(2012)**

14. Jorgensen W.L., Maxwell D.S. and Tirado-Rives J., Development and testing of the OPLS all-atom force field on conformational energetics and properties of organic liquids, *Journal of the American Chemical Society*, https://doi.org/10.1021/ja9621760, **118**, 11225–11236 **(1996)**

15. Kawagishi H., Hamajima K. and Inoue Y., Novel Hydroquinone as a Matrix Metallo-proteinase Inhibitor from the Mushroom, Piptoporus betulinus, *Bioscience, Biotechnology and Biochemistry,* **66**, 2748-2750 **(2002)**

16. Kim S.Y., Song Y.S., Jeong Y.S., Kim E.J. and Kim B.J., Extract of the mycelium of T. matsutake inhibits elastase activity and TPA-induced MMP-1 expression in human fibroblasts, *International Journal of Molecular Medicine,* **34**, 1613-21 **(2014)**

17. Kumar V., Krishna S. and Siddiqi M.I., Virtual screening strategies: Recent advances in the identification and design of anti-cancer agents, *Methods*, https://doi.org/10.1016/j.ymeth.2014.08.010 **(2015)**

18. Khelifa S., Low molecular weight compounds from mushrooms as potential Bcl-2 inhibitors: Docking and Virtual Screening studies **(2016)**

19. Li Y., Liu H. and Xu L., Expression of MMP-9 in different degrees of chronic hepatitis B and its correlation with inflammation, *Experimental and Therapeutic Medicine*, **16**, 4136-4140 **(2018)**

20. Lionta E., Spyrou G., Vassilatis D.K. and Cournia Z., Structure-Based Virtual Screening for Drug Discovery: Principles, Applications and Recent Advances, *Curr Top Med Chem*., **14**, 1923–1938 **(2014)**

21. Lill M.A. and Danielson M.L., Computer-aided drug design platform using PyMOL, *Journal of Computer-Aided Molecular Design*, https://doi.org/10.1007/s10822-010-9395-8, **25**, 13–19 **(2011)**

22. Lee E.J., Kim W.J. and Moon S.K., Cordycepin suppresses TNF-alpha-induced invasion, migration and matrix metalloproteinase-9 expression in human bladder cancer cells, *Phytotherapy Research*, https://doi.org/10.1002/ptr.3132, **24,** 1755–1761 **(2010)**

23. Lee K.R., Lee J.S., Song J.E., Ha S.J. and Hong E.K., Inonotus obliquus-derived polysaccharide inhibits the migration and invasion of human non-small cell lung carcinoma cells via suppression of MMP-2 and MMP-9, *International Journal of Oncology*, **45**, 2533-2540 **(2014)**

24. Lee S.H., Oh I.S., Kim Y.I., Jun S.C., So S.S. and Kim H.G., Phellinus Extracts Inhibit Migration and Matrix Metalloproteinase Secretion in Porcine Coronary Artery Endothelial Cells, *Biotechnology and Bioprocess Engineering*, **12**, 100-105 **(2007)**

25. Lipinski C.A., Lombardo F., Dominy B.W. and Feeney P.J., Experimental and computational approaches to estimate solubility and permeability in drug discovery and development settings, *Advanced Drug Delivery Reviews*, https://doi.org/10.1016/j, **6**, 4–17 **(2012)**

26. Pegu K., Gogoi D., Rai A.K., Bordoloi M. and Bezbaruah R.L., Docking & Virtual Screening of Edible Mushroom Derived Compounds as *Plasmodium falciparum* Triosephosphate Isomerase-Phosphoglycolate Inhibitor, *Indo Global Journal of Pharmaceutical Sciences,* **4**, 29-36 **(2014)**

27. Ramos G.F., Umejiego J.O., Rapales J.J., Awemu G.A., Tejano G.I., Faller E. and Rivers E., GC-MS analysis of bioactive phytochemicals present in methanol extract of P. ostreatus, *Evidence for its Medicinal Diversity*, https://doi.org/10.20959/wjpps201811-12458, **7**, 143–150 **(2018)**

28. Scannevin R.H., Alexander R., Haarlander T.M., Burke S.L., Singer M., Huo C. and Rhodes K.J., Discovery of a highly selective chemical inhibitor of matrix metalloproteinase-9 (MMP-9) that allosterically inhibits zymogen activation, *Journal of Biological Chemistry,* https://doi.org/10.1074/jbc. M117.806075, **292,** 17963–17974 **(2017)**

29. Singh K.D. and Muthusamy K., Molecular modeling, quantum polarized ligand docking and structure-based 3D-QSAR analysis of the imidazole series as dual KT1 and ET A receptor antagonists, *Acta Pharmacologica Sinica*, https://doi.org/10.1038/aps.2013.129, **34**, 1592–1606 **(2013)**

30. Tranchant I., Vera L., Czarny B., Amoura M., Cassar E., Beau F., Stura E.A. and Dive V., Halogen Bonding Controls Selectivity of FRET Substrate Probes for MMP-9, *Chemistry and Biology*, **21**, 408–413 **(2014)**

31. Tripathi S.K., Selvaraj C., Singh S.K. and Reddy K.K., Molecular docking, qpld and adme prediction studies on hiv-1 integrase leads, *Medicinal Chemistry Research*, https://doi.org/10.1007/s00044-011-9940-6, **21**, 4239–4251 **(2012)**

32. Yuan H., Yang P., Zhou D., Gao W., Qiu Z., Fang F., Ding S. and Xiao W., Knockdown of sphingosine kinase 1 inhibits the migration and invasion of human rheumatoid arthritis fibroblast-like synoviocytes by down-regulating the PI3K/AKT activation and MMP-2/9 production in vitro, *Mol Biol Rep*., **41,** 5157–5165 **(2014)**

33. Yeh C.B., Hsieh M.J., Hsieh Y.H., Chien M.H. and Chiou H.L., Antimetastatic Effects of Norcantharidin on Hepatocellular Carcinoma by Transcriptional Inhibition of MMP-9 through Modulation of NF-kB Activity, *PLOS One,* **7**, https://doi.org/10.1371/journal.pone.0031055, e31055 **(2012)**

34. Yves S.P., Julie C. and Céline V.T., Regulation of MMP-9 gene expression for the development of novel molecular targets against cancer and inflammatory diseases, *Expert Opinion on Therapeutic Targets*, DOI: 10.1517/14728222.8.5.473, **8**, 473-489 **(2004)**

35. Zaidman B.Z., Yassin M., Mahajna J. and Wasser S.P., Medicinal mushroom modulators of molecular targets as cancer therapeutics, *Appl Microbiol Biotechnol*., **67**, 453–468 **(2005)**.

(Received 14th February 2020, accepted 15th April 2020)